Trees (2024) 38:1491–1508
https://doi.org/10.1007/s00468-024-02568-9

ORIGINAL ARTICLE

Drought-related mortality, growth and non-structural carbohydrate dynamics in two conifer species during early stages of development

David R. Woodruff[1] · Frederick C. Meinzer[1] · Katherine A. McCulloh[2] · Kimberly O'Keefe[3] · Kelly L. Kerr[4] · Danielle E. M. Ulrich[5] · Johnathan G. Crandall[6]

Received: 26 February 2024 / Accepted: 16 September 2024 / Published online: 14 November 2024

Abstract

To examine the mechanisms associated with growth, survival, and mortality under drought conditions during early developmental stages, physiological and structural parameters were measured on *Pseudotsuga menziesii* (PSME) and *Pinus ponderosa* (PIPO) first-year seedlings grown under two moisture regimes (drought and control) in a common garden experiment. By the end of the 76-day experiment, PSME mortality in the drought and control treatments had reached 30.4% and 11.2%, respectively, while there was only 5.3% mortality in drought PIPO and virtually no mortality in control PIPO. Weekly predawn and mid-day leaf water potential differed significantly between treatments starting ~ mid-way through the study. Although we observed significant differences in photosynthetic gas exchange between species throughout most of the study, there were only minimal differences between treatments within species until the very end of the study. Root, stem, and leaf biomass were significantly greater in PIPO than in PSME throughout the study. PSME seedlings that were dying or recently dead showed a pronounced shift in non-structural carbohydrate (NSC) distribution, with root NSC levels strongly depleted and stem NSC levels increased relative to healthy seedlings. These results suggest a potential role for drought-related constraints on phloem transport in mortality.

Keywords Carbon starvation · Seedling mortality · *Pseudotsuga menziesii* · *Pinus ponderosa*

Introduction

Aridity gradients are a primary determinant of vegetation patterns and species distributions globally (Gentry 1988; Engelbrecht et al. 2007). Climate change is predicted to drive progressively more extreme drought events and heat waves (Meehl and Tebaldi 2004; Seager et al. 2007; Teskey et al. 2015; IPCC 2022, Yuan et al. 2023) and it has the potential to profoundly impact the growth and distribution of tree populations through effects on disturbance regimes, forest productivity, tree mortality, and tree cohort establishment (Brubaker 1986; Scheller and Mladenoff 2005; Gougherty et al. 2021). Species distributions can shift over time through adult mortality and reduced regeneration or through seedling establishment beyond current distribution boundaries, and they are predicted to change greatly in response to future climate change (Araújo and Rahbek 2006; Parmesan 2006; Chmura et al. 2011; Dyderski et al. 2018). Research done on population dynamics of trees indicates that the seedling stage is particularly crucial for the expansion or recession of woody plant species' populations (Hartshorn 1972; Piñero

Communicated by John Major .

✉ David R. Woodruff
david.woodruff@usda.gov

1 USDA Forest Service, Pacific Northwest Research Station, 3200 SW Jefferson Way, Corvallis, OR 97331, USA

2 Department of Botany, University of Wisconsin-Madison, Madison, WI 53705, USA

3 Department of Biology, Northern Michigan University, Marquette, MI 49855, USA

4 Department of Ecology, Evolution, and Marine Biology, University of California, Santa Barbara, CA 93117, USA

5 Ecology Department, Montana State University, Bozeman, MT 59717, USA

6 Laboratory of Genetics, University of Wisconsin-Madison, Madison, WI 53705, USA

et al. 1984; Eriksson and Ehrlen 2008; Urli et al. 2023). Advancing our understanding of the mechanisms involved in early stage seedling mortality and survival in response to increasing drought is, therefore, a key component in developing an ability to more accurately predict potential changes in species distributions.

The early stages of seedling growth involve distinct challenges relative to subsequent stages of tree growth. Younger trees and seedlings generally contain comparatively low levels of non-structural carbohydrates (NSC) on a percent dry matter basis (Lusk and Piper 2007; Woodruff and Meinzer 2011; Maguire and Kobe 2015). Young seedlings, therefore, may be more reliant on NSC reserves during periods when photosynthesis is limited, resulting in depleted NSC. Rooting depth and access to soil horizons with higher water potentials have been shown to be primary determinants of drought survival of woody species (Padilla and Pugnaire 2007; Ovalle et al. 2015; Nardini et al. 2016). Because young seedlings generally have shallow roots, another challenge is that their rooting systems are often confined to soil regions that can reach very low soil water potentials during periods of drought, leaving them vulnerable to tissue dehydration.

Ponderosa pine (*Pinus ponderosa* P. and C. Lawson) is the most widely distributed pine in North America (Burns and Honkala 1990), occurring throughout the western United States, southern Canada, and northern Mexico (Little 1971). Coastal Douglas-fir (*Pseudotsuga menziesii* (Mirb.) Franco var. *menziesii*) grows from west-central British Columbia southward to central California. Both species grow together on either side of the Cascade mountains in Oregon and although the xylem of adult *P. ponderosa* has been shown to be more vulnerable to embolism than that of *P. menziesii* (Piñol and Sala 2000; Domec and Gartner 2002; Stout and Sala 2003; Martinez-Vilalta et al. 2004), *P. ponderosa* typically extends into drier regions than *P. menziesii* (McMinn 1952). These differences in distribution suggest that, despite its resistance to hydraulic dysfunction as an adult, *P. menziesii* may actually be more vulnerable to drought than *P. ponderosa* at the seedling stage, potentially limiting its range for establishment and survival.

In this study, we examined drought vulnerability at very early seedling developmental stages for *P. menziesii* (PSME) and *P. ponderosa* (PIPO). Our objectives were to determine if constraints on seedling growth were more closely associated with dehydration or reduced carbon availability either caused by whole plant or localized reductions, and to determine the degree to which each of these mechanisms may be associated with seedling mortality. We created experimental drought treatments in raised beds of relatively large volumes to simulate field soil conditions. The objective was to simulate a natural progression of water stress as opposed to an abrupt onset of extreme drought conditions, which is common in experiments that involve potted plants with limited vertical and lateral access to soil. We hypothesized that: (1) PIPO survival and growth would be greater than that of PSME due to the contrasting moisture regimes within their relative ranges; and that within species, survival and growth would be greater for seedlings from drier seed sources; (2) seedling growth and survival would be correlated with gas exchange and hydraulic characteristics; (3) NSC would become depleted in seedlings most affected by drought stress; and (4) that the abundance or depletion of NSC in different organs would provide information about the mechanistic nature of mortality or growth constraints associated with drought stress in young PSME and PIPO seedlings (e.g., carbon starvation, phloem transport limitation).

Materials and methods

Study site

This study was conducted in four raised soil beds (18.3 m-long × 1.5-m-wide x ~ 0.75 m-deep) on the Oregon State University campus located in Corvallis, OR from March to October of 2014. The raised beds were covered using clear polycarbonate panels installed in a manner that excluded precipitation from the beds yet allowed sufficient air ventilation to avoid excessive heat build-up. Seeds for both species were selected from both dry and wet sources. Dry source PIPO seeds were from an area near Spray OR (44.834306°N, 119.79449°W; mean annual precipitation: 339 mm; mean annual daily temperature: 11.2 °C). Wet source PIPO seeds were from a mix of seed sources from the Willamette Valley, spanning from the junction of the Columbia and Willamette Rivers to south of Eugene, OR. For this population, the climate was estimated to be similar to that of Corvallis, OR (44.564566°N, 123.262044°W; mean annual precipitation: 1059 mm; mean annual daily temperature: 11.37 °C). Dry source PSME seeds were from sites near Cottage Grove, OR (43.797247°N, 123.059064°W, mean annual precipitation: 1133 mm, mean annual temperature: 11.04 °C). Wet source PSME seeds were from sites near Hebo, OR (45.229301°N, 123.859466°W, mean annual precipitation: 2385 mm; mean annual temperature: 10.41 °C). Climate data were obtained from PRISM Climate Group at Oregon State University; all climate data from years: 1895–2023. Seeds were stratified in February of 2014, planted in a greenhouse in March of 2014, and then transplanted to raised beds in June of 2014. Prior to transplanting, the raised beds were sterilized with a soil fumigant (Basamid Granular Certis USA, Columbia, MD) and rototilled to ensure even coverage. Following fumigation, the beds were leveled to create an even surface for planting and a mycorrhizal inoculum (Great White Premium Mycorrhizae, Plant Success, http://www.plant-success.com) was applied to

the beds according to the label. Due to experimental limitations (i.e., each bed could only receive one water treatment), PIPO and PSME were planted across each bed to minimize the potential spatial variation in growth conditions experienced by each species. To do so, each of the four beds was divided into thirds and each of these bed-thirds was further divided into two sections, resulting in six sections per bed and 24 total sections. The PIPO and PSME seedlings were randomly assigned to sections within bed-thirds and planted in five rows across the width of the section (11 seedlings per row planted 15 cm apart), which resulted in 55 seedlings per bed section, for a total of 1320 seedlings, although not all seedlings persisted following transplanting from the greenhouse. At the beginning of the study there were 376 control PSME, 362 drought PSME, 258 control PIPO and 244 drought PIPO seedlings.

Drought treatment

The seedlings were watered daily following planting in raised beds in mid-June until day of year (DOY) 206 (July 25) when the treatments were imposed. Then, two beds were randomly selected to receive the drought treatment, while the remaining two beds received the control treatment. Evaporation data were collected at the Hyslop Field Lab Weather Station located in Corvallis, OR. Drought beds were left un-watered and control beds were watered once a week and received 25% of the average weekly potential evapo-transpiration for the duration of the study. The amount of water applied was calculated as a percentage of the potential evaporation over 3 days prior to watering.

Soil and seedling water potentials

Gypsum block soil matric potential sensors (223L, Campbell Scientific, Logan, UT) were installed in the beds and values were recorded every 30 min with a data logger (CR10X, Campbell Scientific). Two soil sensors were installed one-third of the length of the bed from each bed end. At each of these locations, one sensor was installed at a depth of 10 cm and the other at 20 cm. The water potential threshold for the lower end of the soil sensors is − 1.0 MPa, so the true values for the most negative mean soil water potential values were likely biased upwards. Measurements of leaf water potential (Ψ_l) were conducted with a pressure chamber (PMS Instrument Company, Albany, OR, USA) on whole seedling shoots which had been bagged in the dark for 5 min to remove within seedling gradients in water potential. Predawn (~ 0515 to ~ 0700 standard time) and mid-day (~ 1300 to ~ 1430 standard time) measurements of Ψ_l were conducted on four individuals (from four distinct randomly selected sections) per treatment, per species from both seed sources during each measurement session (32 per session). Measurements occurred on DOY 206, 212, 219, 233, 240, 247, 259, 275 and 282, of year 2014. A total of 136 destructive water potential readings occurred per species over the course of the study.

Gas exchange

Morning (~ 0830 to ~ 1000 standard time) and afternoon (~ noon to ~ 1330 standard time) gas exchange were measured with a portable photosynthesis system with 2 × 3 cm chamber equipped with a red and blue LED source and CO_2 injector (LI-6400; Li-Cor, Lincoln, NE, USA) for both species on nine different dates between DOY 206 and 282. Reference [CO_2] was maintained at 400 ppm to match current ambient [CO_2] (NOAA Global Monitoring Division, https://www.esrl.noaa.gov/gmd/ccgg/trends/), and the flow rate was kept at 500 µmol s^{-1}. Leaf temperature was set to match ambient conditions and cuvette irradiance was set to 1200 µmol m^{-2} s^{-1}. Groups of needles were isolated on shoots for gas-exchange measurements and later scanned for leaf area. Photosynthesis and stomatal conductance (g_s) values were normalized by one-sided leaf areas using a scanner and ImageJ Version 1.27 image analysis software (Abramoff et al. 2004). Measurements were conducted on four individuals per treatment, per species from both seed sources, during each measurement session. Measurements occurred on DOY 206, 212, 219, 233, 240, 247, 259, 275 and 282, of year 2014. A total of 72 destructive gas exchange measurements were done per species over the course of the study.

Hydraulic conductivity

Hydraulic conductivity was measured on PSME stem segments at the University of Wisconsin–Madison following the end of the growing season (February 2015). Seedling specific hydraulic conductivity (K_s) and leaf specific conductivity (K_l) were both measured in PSME but not in PIPO due to the lack of a substantial treatment effect on mortality in PIPO. Entire above-ground portions of seedlings were collected early in the morning, wrapped in damp paper towels, double-bagged, packed into boxes that also contained a blue ice block, and shipped overnight from Corvallis, OR to Madison, WI. Samples were measured within 4 days of harvest. Stem segments were cut from the shoot underwater using fresh razor blades. The length of the final segments on average (SE) was 2.1 (0.7) cm. To refill any embolisms that had been present in the seedling in situ or that had been introduced during sample preparation, segments were vacuum infiltrated overnight. The solution used for infiltration and measurement was an aqueous solution of 20 mM KCl that had been filtered using 0.2 µm filter paper. To measure segment hydraulic conductivity, the basal end of a segment was connected via tubing to a reservoir of measurement solution

roughly 65 cm above the stem segment. The distal end of the segment was connected via tubing to an electronic balance (Entris 224-1 s, Sartorius Corp, Bohemia, NY), which was connected to a computer. Background volume flow rates were recorded before and after measuring the volume flow rate through the segment, while it was exposed to the elevated water reservoir. The computer recorded the change in water mass every 2 s and calculated the volume flow rate with the R-based program, conductR (https://uwmadison.app.box.com/v/conductR). The average volume flow rate was recorded every five measurements and once flow had stabilized, the average volume flow rate was divided by the pressure inducing flow to calculate hydraulic conductance (K_h). Segment length-specific hydraulic conductivity (k_s) was determined as $k_s = (K_h * l)/A_s$, where l is the segment length and A_s is the cross-sectional area of the stem (without bark). Leaf-area-specific conductivity (k_L) was also determined as $k_L = (K_h * l)/A_L$, where A_L is the leaf area supported by the stem segment. The dry masses of leaves supplied by the stem segments were determined after drying the needles in an 80 °C oven for 2 days. An allometric relationship between leaf mass and area was developed by measuring leaf area and mass on a subset of samples, following which A_L was determined from the segment leaf mass and this allometric relationship.

Seedling sampling, mortality and decline

Seedlings were harvested to monitor root and shoot biomass approximately every 1–2 weeks throughout the study. At each sampling period, 8–20 seedlings from each treatment and species were harvested. All samples were sealed into plastic bags and immediately placed into a cooler with ice for transport to the nearby laboratory. In the laboratory, samples were placed into a coin envelope and kept in a 65 °C oven until dry. A visual estimate of percent of foliar browning was also recorded every 1–2 weeks for all seedlings. Any seedling (from control or drought treatments) with 100% green foliage was categorized as being healthy. All seedlings with browning or highly chlorotic foliage were categorized as dead/dying, assigned a % value of dying foliage via visual assessment, and collected for additional biomass and NSC analyses. The vast majority of dead/dying seedlings had foliage that was 100% brown and/or highly chlorotic (100% brown for both PIPO control and drought; 95% and 98% brown for PSME control and drought, respectively). Healthy seedlings sampled for measurement were included in healthy seedling counts throughout the duration of the study.

Chemical analyses

Samples for NSC analyses were taken from those collected for biomass analyses (see above). NSC samples collected in the afternoon (~ noon to ~ 1330 standard time) and were immediately placed on dry ice in a cooler at the raised beds and temporarily stored in a – 20 °C freezer before being microwaved for 45–120 s (depending on the size of the sample) with a 1000 W microwave to stop all enzymatic activity. They were then oven dried for ~ 72 h at 65 °C and ground to a fine powder using a VWR high throughput hard tissue homogenizer. Dried and ground samples of needles, stem, and roots were analyzed for the content of sucrose, glucose + fructose, starch, and total NSC. Although these do not constitute the entire complement of NSCs in plants, the majority of studies assessing NSCs focus on these, and they are the predominant NSCs available for use by temperate forest trees (Hoch et al. 2003). Water was added to the powdered samples and NSC was extracted from the solutions by heating them in steam for 1.5 h. The concentration of free glucose was determined photometrically on a 96-well microplate photometer (Multiskan FC; Thermo Scientific, Waltham, MA, USA) after enzymatic conversion of glucose to gluconate-6-phosphate. Photometric analysis was based on the absorbance of samples at 340 nm in solution with reference to the absorbance of a glucose reference solution. Samples were analyzed both before and after enzymatic treatments of sucrose digestion by invertase for 45 min and starch digestion by amyloglucosidase overnight. Glucose + fructose content was determined from photometric analysis of sample solutions with no enzymatic treatment. Sucrose content was determined by subtracting the glucose + fructose content from the photometric analysis of the glucose concentration of sample solutions following invertase enzyme treatment. Total NSC was determined from the amyloglucosidase reaction mixture, which contains the original concentrations of free glucose and fructose, plus glucose and fructose liberated from starch and sucrose. Inclusion of sucrose standards in each set of samples subjected to amyloglucosidase treatment indicated that amyloglucosidase hydrolyzed sucrose as well as starch. The starch content was determined by subtracting the glucose content of the sample solution following invertase enzyme treatment from the total NSC content. NSC amounts are reported as % dry matter of whole tissue for content and as milligrams for pools within individual seedling components (i.e., roots, stems or foliage). Concentrations of all NSC components are expressed on a % dry mass basis. Pool values were determined by multiplying % dry matter by the masses of seedling components. NSC concentrations and pools were compared between healthy (those with no signs of browning foliage) and dead/dying (those with some or all foliage browning) in PSME seedlings, but not in PIPO seedlings due to the limited amount of mortality in PIPO.

Statistical methods

All statistical analyses were performed in Program R V3.3.3 (R Core Team 2017). For all analyses, we checked for normality using normal qq-plots and assessed homogeneity of variances by examining residuals vs. fitted plots (Faraway 2005). Data were log- or square root-transformed as needed. In addition, individual seedlings were assumed to be independent for all analyses, because (1) both species were planted within each bed to minimize spatial variation in growth conditions across individuals (as described in Sect. Study Site) and (2) mixed effects models were used to further account for random effects associated with individual beds and seedling positions within bed (Harrison et al. 2018). Differences in soil water potential across water treatments, soil depth, DOY and their interactions were assessed using a linear fixed effects model:

$$y \sim \text{water} * \text{depth} * \text{DOY} \quad (1)$$

Differences among treatment contrasts for leaf water potential, gas exchange, and biomass parameters were assessed using linear mixed effects models. Separate models were run for each parameter with water treatment, species, DOY, and their interactions, as well as seedling population as fixed effects:

$$y \sim (\text{water} * \text{species} * \text{DOY}) + \text{population} + (1|\text{bed}) + (1|\text{position}) \quad (2)$$

Differences among water treatments and populations were also assessed for seedling- and leaf-specific hydraulic conductivity using linear mixed effects models:

$$y \sim \text{water} + \text{population} + (1\text{bed}) + (1\text{position}) \quad (3)$$

Bed and position within bed were included as random effects for all mixed effects analyses.

Two different linear mixed effects models were used to assess differences among treatment contrasts for both NSC concentrations and NSC pools. First, we compared differences in NSC concentrations among species, water treatments, tissue type, and their interactions for all individuals sampled on DOY 247. Bed and position within bed were included as random effects and population was included as an additive fixed effect:

$$y \sim (\text{water} * \text{species} * \text{tissue}) + \text{population} + (1|\text{bed}) + (1|\text{position}) \quad (4)$$

Second, we compared differences among water treatments, tissue type, and health status ("healthy" vs. "dead/dying" individuals) for PSME sampled on multiple days at the end of the experiment, with population included as an additive fixed effect and bed, position, and date included as random effects:

$$y \sim (\text{water} * \text{tissue} * \text{health}) + \text{population} + (1|\text{bed}) + (1|\text{position}) + (1|\text{date}) \quad (5)$$

A separate analysis was also conducted to compare PSME whole-plant NSC pools across water treatments, health status and their interactions, with population included as an additive effect and bed, position within bed, and sampling date were included as random effects:

$$y \sim (\text{water} * \text{health}) + \text{population} + (1|\text{bed}) + (1|\text{position}) + (1|\text{date}) \quad (6)$$

For both NSC concentration and NSC pool analyses, separate analyses were run for each NSC component (total NSC, starch, and sugars).

Finally, a logistic regression model was used to compare plant mortality across species, water treatments, their interactions, as well as population and day of year:

$$y \sim (\text{species} * \text{water}) + \text{DOY} + \text{population} + (1|\text{bed}) + (1|\text{position}) \quad (7)$$

Bed and position within bed were included as random effects, and day of year was log-transformed. Log estimates and estimated odds ratios of mortality for main effects in respect to baseline model conditions are reported and were used to estimate mortality ratios of both PIPO and PSME under drought vs. control conditions. For PIPO, the estimated mortality ratio under drought equals the odds ratio of mortality for the drought treatment in respect to the baseline model condition, "PIPO." For PSME, the estimated mortality ratio under drought was calculated by multiplying the odds ratio of PIPO mortality under drought by the odds ratio of the PSME * drought interaction.

Results

Soil water potential

Droughted beds experienced significantly lower soil water potentials compared with the control beds and the treatment effects increased throughout the study differently for each soil depth ($p = 0.03$; Table 1). Droughted beds had a mean soil water potential of − 0.55, − 0.83 and − 0.9 MPa at the 10 cm depth for DOY 228, 248 and 268, respectively (Fig. 1a). Control beds had higher soil water potentials at the 10 cm depth with mean values of − 0.07, − 0.04, and − 0.05 MPa for these same respective days (Fig. 1a). At the 20 cm depth, droughted beds had a mean soil water potential of − 0.28, − 0.35 and − 0.34 MPa for DOY 228,

Table 1 Linear fixed effects model comparing soil water potential across water treatments (Water), soil depth (Depth), day of year (DOY), and their interactions

Variable	DF	SS	MS	F	*P*
Soil water potential[1]					
Water	1	278.45	278.45	3624.52	< 0.01*
Depth	1	18.44	18.44	240.04	< 0.01*
DOY	1	5.829	5.83	75.88	< 0.01*
Water * Depth	1	8.90	8.90	115.90	< 0.01*
Water * DOY	1	8.91	8.91	116.00	< 0.01*
Depth * DOY	1	2.48	2.48	32.32	< 0.01*
Water * Depth * DOY	1	0.38	0.38	4.93	0.03*
Residuals	230	17.67	0.08		

F and *P* values for the main effects and their interactions. An asterisk (*) indicates significance at the $\alpha = 0.05$ level

DF degrees of freedom, *SS* sum of squares, *MS* mean squares

[1]Log-transformed data

248 and 268, respectively (Fig. 1b); and respective water potentials values for the same days at the 20 cm depth in the control beds were − 0.05, − 0.05 and − 0.05 MPa (Fig. 1b). The maximum negative range of the soil sensors was − 1.0 MPa, so later mean values of the droughted beds at the 10 cm depth include readings that were outside of the range of the sensors. Actual mean soil water potential values in these cases are expected to have been slightly lower than the values provided by the sensors.

Seedling water potential

Predawn and mid-day leaf water potential were generally lower in droughted seedlings than control seedlings, and these treatment differences increased through time ($p < 0.01$ and $p = 0.04$ for predawn and mid-day leaf water potential, respectively; Table 2; Fig. 1c, d). Both predawn and mid-day water potential also differed significantly between species. PSME exhibited significantly lower predawn water potentials than those of PIPO, as well as lower mid-day water potentials than PIPO on certain measurement dates ($p < 0.01$ for both predawn and mid-day water potential; Table 2; Fig. 1c, d).

Seedling biomass

Although above- and belowground biomass increased throughout time, each component differed among species and treatments throughout the majority of the study (Fig. 2). Leaf biomass ($p < 0.01$) and root:shoot ($p = 0.03$) differed significantly between species, although this varied through time with PIPO having greater leaf biomass and PSME having greater root:shoot towards the end of the experiment (Table 3; Fig. 2). Stem biomass ($p < 0.01$), root biomass ($p = 0.01$), and total biomass ($p < 0.01$) were consistently greater in PIPO than PSME throughout the experiment (Table 3). Leaf biomass, root biomass, and total biomass were all significantly lower in all droughted seedlings than control seedlings by the end of the experiment (significant Water * DOY effect; Table 3). Leaf,

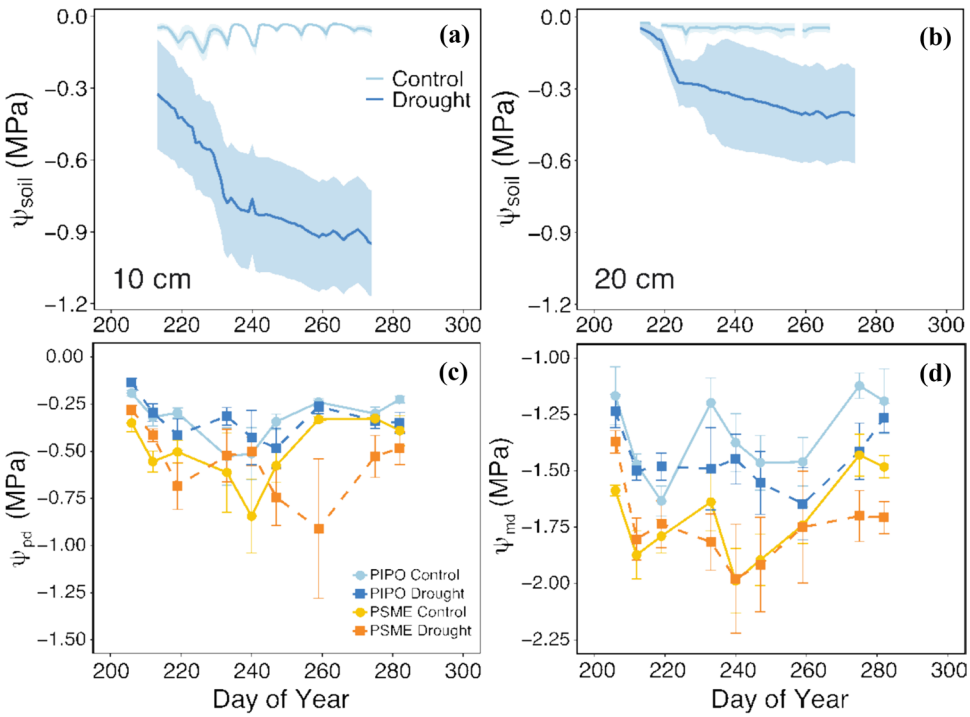

Fig. 1 Mean soil water potential measured at 10 cm (**a**) and 20 cm (**b**) depths, for control and drought treatments. Shading indicates ± 1 SEM. Also shown are (**c**) predawn and (**d**) mid-day leaf water potential measured for PIPO and PSME throughout the experiment. Leaf water potential values are means (± 1 SEM) for control (solid lines) and drought (dotted lines) treatments. The water potential threshold for the lower end of the soil sensors is − 1.0 MPa. Corresponding statistics are shown in Table 1

Table 2 Linear mixed effects models comparing leaf water potential across water treatments (Water), species (Species), day of year (DOY), and their interactions, as well seedling population (Population)

Variable	SS	MS	DF_{Num}	DF_{Den}	F	*P*
Predawn water potential[1]						
Water	0.001	0.001	1	2.01	0.01	0.92
Species	4.47	4.47	1	78.54	42.08	< 0.01*
DOY	7.85	0.98	8	183.13	9.23	< 0.01*
Population	1.08	1.08	1	76.01	10.12	< 0.01*
Water * Species	0.001	0.001	1	78.54	0.01	0.92
Water * DOY	2.89	0.36	8	183.13	3.40	< 0.01*
Species * DOY	1.38	0.17	8	183.12	1.62	0.12
Water * Species * DOY	0.23	0.03	8	183.13	0.27	0.98
Mid-day water potential[1]						
Water	0.01	0.01	1	2.00	0.26	0.66
Species	1.30	1.30	1	75.15	56.47	< 0.01*
DOY	1.50	0.19	8	192.05	8.14	< 0.01*
Population	0.27	0.27	1	72.40	11.94	< 0.01*
Water * Species	0.02	0.02	1	75.18	0.94	0.34
Water * DOY	0.39	0.05	8	192.07	2.10	0.04*
Species * DOY	0.25	0.03	8	192.05	1.38	< 0.01*
Water * Species * DOY	0.16	0.02	8	192.06	0.87	0.55

Bed and position within bed were included as random effects. *F* and *P* values for the main effects and their interactions. An asterisk (*) indicates significance at the $\alpha = 0.05$ level

SS sum of squares (SS), *MS* mean squares (MS), DF_{Num} numerator degrees of freedom, DF_{Den} denominator degrees of freedom

[1]Log-transformed data

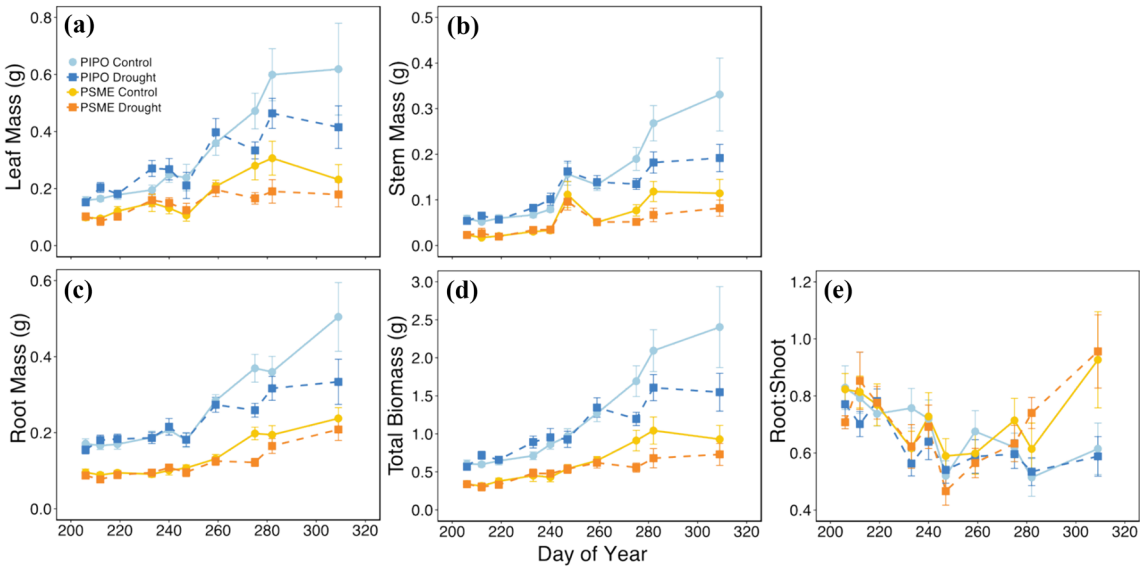

Fig. 2 Plant biomass components measured for PIPO and PSME throughout the experiment. Shown are mean (±1 SEM) leaf mass (**a**), stem mass (**b**), root mass (**c**), total biomass (**d**), and root-to-shoot ratio (**e**) for control (solid lines) and drought (dotted lines) treatments. Corresponding statistics are shown in Table 3

stem, and root biomass were 29%, 29%, and 30% lower, and root:shoot biomass was 4% lower in droughted PIPO compared to control PIPO by DOY 275 (Fig. 2). On the same date, leaf, stem, and root biomass were 41%, 33%, and 38% lower, and root:shoot biomass was 11% lower in droughted PSME compared to control PSME (Fig. 2).

Table 3 Linear mixed effects models comparing biomass across water treatments (Water), species (Species), day of year (DOY), and their interactions, as well seedling population (Population)

Variable	SS	MS	DF_{Num}	DF_{Den}	F	*P*
Leaf mass						
Water	0.02	0.02	1	4.41	0.87	0.40
Species	1.06	1.06	1	90.50	63.12	< 0.01*
DOY	4.33	0.48	9	526.09	28.70	< 0.01*
Population	0.11	0.11	1	86.23	6.25	0.01*
Water * Species	0.0001	0.0001	1	97.91	0.01	0.94
Water * DOY	0.43	0.05	9	526.50	2.85	< 0.01*
Species * DOY	0.82	0.09	9	526.04	5.44	< 0.01*
Water * Species * DOY	0.07	0.01	9	526.43	0.48	0.89
Stem mass[1]						
Water	0.37	0.37	1	3.14	1.32	0.33
Species	50.68	50.68	1	86.05	180.14	< 0.01*
DOY	129.09	14.34	9	523.55	50.98	< 0.01*
Population	0.19	0.19	1	81.78	0.66	0.42
Water * species	0.09	0.09	1	92.41	0.31	0.58
Water * DOY	4.58	0.51	9	524.20	1.81	0.06
Species * DOY	3.14	0.35	9	523.48	1.24	0.27
Water * species * DOY	0.29	0.03	9	524.13	0.11	0.99
Root mass[2]						
Water	0.02	0.02	1	2.50	3.85	0.16
Species	1.68	1.68	1	85.70	282.64	< 0.01*
DOY	2.13	0.24	9	545.39	39.75	< 0.01*
Population	0.00002	0.00002	1	79.13	0.004	0.95
Water * species	0.00005	0.00005	1	90.81	0.01	0.93
Water * DOY	0.14	0.02	9	545.74	2.53	0.01*
Species * DOY	0.09	0.01	9	545.39	1.63	0.10
Water * Species * DOY	0.03	0.003	9	545.78	0.56	0.83
Total biomass[1]						
Water	0.14	0.14	1	5.63	1.11	0.34
Species	18.90	18.90	1	89.57	154.54	< 0.01*
DOY	56.54	6.28	9	518.31	51.363	< 0.01*
Population	0.44	0.44	1	86.20	3.56	0.06
Water * Species	0.09	0.09	1	97.48	0.76	0.39
Water * DOY	2.52	0.28	9	518.8	2.29	0.02*
Species * DOY	1.33	0.15	9	518.25	1.21	0.29
Water * Species * DOY	0.57	0.06	9	518.71	0.52	0.86
Root:shoot[2]						
Water	0.002	0.002	1	4.92	0.13	0.74
Species	0.03	0.03	1	86.23	1.77	0.19
DOY	1.73	0.19	9	519.43	11.14	< 0.01*
Population	0.09	0.09	1	82.55	5.07	0.03*
Water * species	0.003	0.003	1	93.88	0.16	0.69
Water * DOY	0.10	0.01	9	519.83	0.66	0.75
Species * DOY	0.32	0.04	9	519.37	2.04	0.03*
Water * species * DOY	0.18	0.02	9	519.75	1.13	0.34

Bed and position within bed were included as random effects. *F* and *P* values for the main effects and their interactions. An asterisk (*) indicates significance at the $\alpha = 0.05$ level

SS sum of squares, *MS* mean squares, DF_{Num} numerator degrees of freedom, DF_{Den}denominator degrees of freedom

[1]Log-transformed data

[2]Square root-transformed data

Table 4 Logistic regression comparing plant mortality across species, water treatments, their interactions, as well as seedling population and day of year

Variable	Estimated coefficient	SE	Estimated odds ratio	*P*
Mortality				
(Intercept)	− 14.59	1.15	4.62e-07	< 0.01*
PSME	4.59	1.00	98.39	< 0.01*
Drought	2.36	1.18	10.53	0.04*
Dry Population	1.09	0.49	2.98	0.03*
DOY	3.21	0.20	24.81	< 0.01*
PSME * Drought	-0.30	1.17	0.74	0.80

Bed and position within bed were included as random effects. Estimated odds ratio, and *P* values for the model intercept, the main effects compared to baseline effects (PIPO, control conditions, and the wet population), and their interaction. An asterisk (*) indicates significance at the $\alpha = 0.05$ level

SE standard errors

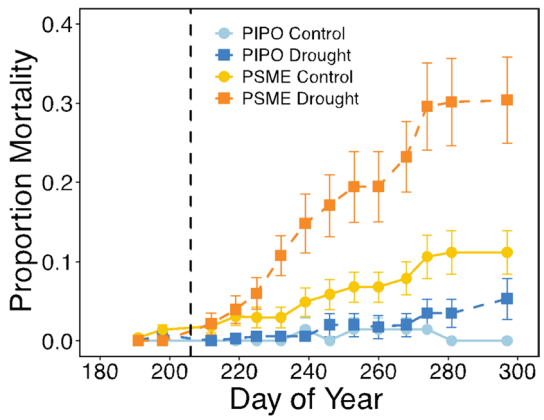

Fig. 3 Plant mortality measured for PIPO and PSME throughout the experiment. Shown are mean (±1 SEM) proportion of dead/dying seedlings for control and drought treatments. The dashed line indicates the beginning of the drought treatment. Corresponding statistics are shown in Table 4

Seedling mortality

Seedling mortality increased significantly through time, for both species and water treatments, so that the odds of mortality increased by a multiplicative factor of 24.81 from the beginning to the end of the experiment ($p < 0.01$; Table 4). Baseline mortality was substantially greater in PSME than PIPO, resulting in overall greater absolute seedling mortality in both drought and control PSME by the end of the experiment (Fig. 3). By DOY 297 (late October), PSME mortality in the drought and control treatments had reached 30.4% and 11.2%, respectively. In contrast, mortality of PIPO was substantially lower, only reaching about 5% in the drought treatment and negligible in the control treatment, respectively (Fig. 3). The ratio of mortality in drought vs. control conditions was 10.54 for PIPO and 7.79 for PSME, indicating that the effect of drought on mortality was proportionally greater for PIPO than for PSME when compared to their respective baseline (control) mortality levels (Table 4; Fig. 3).

Gas exchange and hydraulic conductivity

Both stomatal conductance and photosynthesis were significantly greater in PIPO than in PSME throughout most of the study ($p < 0.01$ for both stomatal conductance and photosynthesis; Table 5; Fig. 4). While stomatal conductance did not differ between water treatments within species, photosynthetic rates varied by treatment through time ($p < 0.01$) and were greater in control seedlings by the end of the experiment (Fig. 4a). K_s of PSME seedlings were 0.18 mg mm^{-1} s^{-1} kPa^{-1} (SE = 0.02) and 0.17 mg mm^{-1} s^{-1} kPa^{-1} (SE = 0.03) for the control and droughted treatments, respectively ($p = 0.85$; Table 6). K_l was also not significantly different between treatments in the PSME seedlings ($p = 0.46$; Table 6).

Non-structural carbohydrates

NSC concentrations and pools differed among plant tissues and species on DOY 247 (Fig. 5), but not treatments (data not shown). Total NSC and starch concentrations were greater in leaves than roots or stems, but only for PSME ($p < 0.01$ for both starch and total NSC; Table 7; Fig. 5a, c). Sugar concentrations were lower in roots than leaves in both species ($p < 0.01$; Table 7; Fig. 5b). NSC pools were generally greater in leaves than in stems or roots for both species, particularly for total NSC ($p < 0.01$; Table 7; Fig. 5f) and PSME starch pools ($p < 0.01$; Table 7; Fig. 5d). PIPO had greater root and stem starch pools, leaf, root, and stem sugar pools, and root and stem total NSC pools than PSME ($p < 0.01$ for each; Table 7; Fig. 5d–f).

When compared across healthy (those with no signs of browning foliage) vs. dead/dying (those with some or all foliage browning) PSME seedlings, starch, sugar, and total NSC concentrations and pools all exhibited significant tissue x health status interactions ($p < 0.01$ for each; Table 8; Fig. 6). With the exception of leaf starch concentrations, leaf and stem NSC concentrations were lower in healthy individuals compared to dead/dying individuals (Fig. 6a–c). Conversely, root NSC concentrations were greater in healthy individuals than dead/dying individuals (Fig. 6a–c). Similar patterns were observed in stem and root NSC pools (Fig. 6d). Total NSC content was significantly higher in dead/dying PSME stems and healthy

Table 5 Linear mixed effects models comparing leaf gas exchange across water treatments (Water), species (Species), day of year (DOY), and their interactions, as well seedling population (Population)

Variable	SS	MS	DF_{Num}	DF_{Den}	F	*P*
Photosynthesis						
Water	3.21	3.21	1	2.01	0.20	0.70
Species	2176.00	2176.00	1	70.30	132.88	< 0.01*
DOY	880.91	110.11	8	457.58	6.72	< 0.01*
Population	0.36	0.36	1	67.20	0.02	0.88
Water * Species	4.99	4.99	1	70.32	0.31	0.58
Water * DOY	618.77	77.35	8	457.56	4.72	< 0.01*
Species * DOY	550.09	68.76	8	457.59	4.20	< 0.01*
Water * Species * DOY	190.69	23.84	8	457.58	1.46	0.17
Stomatal conductance[1]						
Water	0.01	0.01	1	2.02	0.578	0.53
Species	0.56	0.56	1	69.85	67.80	< 0.01*
DOY	1.07	0.13	8	452.70	16.27	< 0.01*
Population	0.01	0.01	1	67.07	0.83	0.37
Water * Species	0.00002	0.00002	1	69.85	0.003	0.96
Water * DOY	0.13	0.02	8	452.67	1.89	0.06
Species * DOY	0.19	0.02	8	452.68	2.86	< 0.01*
Water * Species * DOY	0.10	0.01	8	452.68	1.55	0.14

Bed and position within bed were included as random effects, *F* and *P* values for the main effects and their interactions. An asterisk (*) indicates significance at the $\alpha = 0.05$ level

SS Shown are sum of squares, *MS* mean squares, DF_{Num} numerator degrees of freedom, DF_{Den} denominator degrees of freedom

[1]Square root-transformed data

PSME roots compared to their healthy and dead/dying counterparts, respectively ($p < 0.00001$ for both; Fig. 6d), while the somewhat higher total NSC content in foliage of dead/dying seedlings compared to the healthy seedlings was not significant ($p = 0.067$). Starch content of dead/dying seedlings was significantly higher in stems ($p = 0.01$) and significantly lower in roots ($p = 0.03$) but not significantly different in foliage compared to healthy seedlings. Sugar content was significantly different in all three organs with sugar content of roots substantially lower in the dead/dying seedlings ($p < 0.00001$) and substantially higher in the stems and foliage of dead/dying seedlings ($p < 0.00001$ for both, Fig. 6). Mean whole seedling NSC pools were nearly identical in dead/dying and healthy PSME seedlings (25.6 mg (SE = 2.1) and 26.0 mg (SE = 3.4), respectively, $p = 0.92$; Fig. 6d). Mean leaf NSC pools were not significantly different between dead/dying and healthy seedlings, but the mean stem NSC pool was significantly lower in the healthy seedlings ($p = 0.023$, Fig. 6d). The most striking difference in NSC pools was in the roots, with the dead/dying seedlings having only a sixth of the mean NSC pool size as that of the healthy seedlings ($p < 0.0001$; Fig. 6d).

Population

A number of factors were significantly influenced by seed source, including pre-dawn and mid-day water potential, leaf mass, root:shoot, mortality and starch concentration in PSME. Pre-dawn and mid-day water potential was ~ 0.1 MPa, and 0.15 MPa (respectively) more negative in dry seed source populations ($p < 0.01$, Table 2). Leaf mass of seedlings from wet seed source populations were ~ 0.04 g greater than those of dry seed sources ($p = 0.01$, Table 3) and root:shoot of dry seed source seedlings was ~ 0.06 greater than those of wet seed source populations ($p = 0.03$, Table 3). Logistic regression analyses indicated that mortality in the dry populations was 2.93 times more likely under drought than the control treatment, and mortality in the wet populations was 2.21 times more likely under drought than the control treatment ($p = 0.03$, Table 4). Starch concentration of PSME seedlings from dry seed source populations were almost 1.2% greater than those from west sources ($p = 0.02$, Table 8).

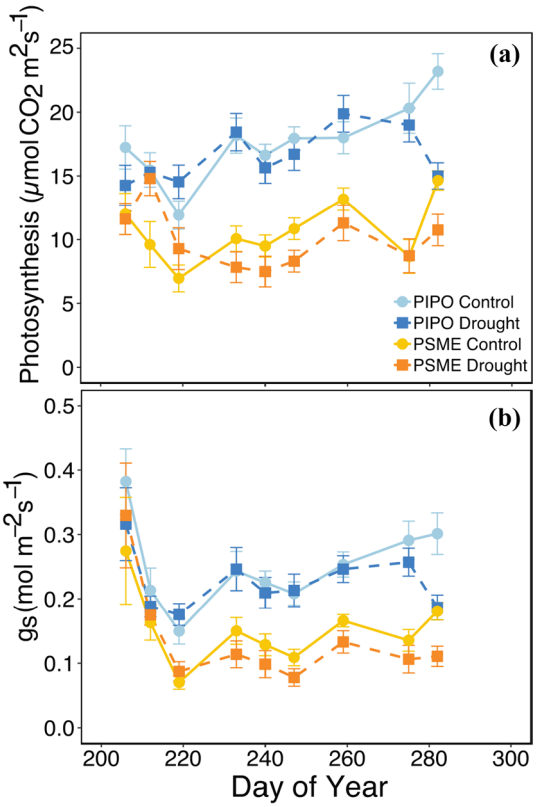

Fig. 4 Leaf gas exchange measured for PIPO and PSME throughout the experiment. Shown are mean (±1 SEM) photosynthesis (**a**) and stomatal conductance (g_s; **b**) for control (solid lines) and drought (dotted lines) treatments. Corresponding statistics are shown in Table 5

Discussion

Due to its range extending into drier regions (McMinn 1952), we anticipated that PIPO survival and growth would be greater than that of PSME under drought conditions. Indeed, PSME experienced significantly more drought-associated mortality than PIPO and the mortality started much earlier in the growing season (Fig. 3). Despite their substantial differences in survival, both species experienced comparable levels and timing of reduced growth under water limitation (Fig. 2). The lack of significant differences in seedling water potential values between treatments earlier in the study, despite substantial differences in other measures such as mortality (see below), may to some extent be attributable to the unavoidable culling of more water stressed seedlings in the drought treatments as those seedlings died or began to decline, thereby essentially eliminating those seedlings from the analyses.

The influence of seed source on pre-dawn and mid-day water potentials, biomass variables such as leaf mass and root:shoot, and starch concentration in PSME, likely reflect adaptations driven by environmental factors in the respective environments. Although we expected seed source to have less of an impact on mortality than species, we were surprised by the greater effect of the drought treatment on seedlings from dry seed sources than wet sources (Table 4). In a study comparing physiological characteristics of PIPO seedlings from dry and mesic seed sources, Kerr et al. (2015) found that PIPO seedlings from dry sources exhibited more conservative behavior, suggesting that in these seedlings increased resistance to drought and extreme temperatures was favored over more rapid growth. It is possible that in the current study, enhanced growth was more beneficial for seedling survival, particularly with regards to root growth (see below).

These growth and mortality responses to water stress reflect the differences in early stage challenges for survival between these two species. PIPO typically germinates in relatively open stands following fire with little understory competition yet lower water availability, while PSME often germinates with more severe understory competition and greater water availability (Franklin and Dyrness 1988). The question then is: mechanistically, how are PIPO seedlings able to survive drought better than PSME? PIPO was able

Table 6 Linear mixed effects models comparing PSME seedling specific conductivity (K_s) and leaf specific conductivity (K_l) across water treatments (Water) and seedling population (Population)

Variable	SS	MS	DF_{Num}	DF_{Den}	F	*P*
K_s [1]						
Water	0.01	0.01	1	1.98	0.05	0.85
Population	0.12	0.12	1	27.06	0.49	0.49
K_l [1]						
Water	0.36	0.36	1	1.79	0.85	0.46
Population	0.11	0.11	1	23.35	0.24	0.63

Bed and position within bed were included as random effects, *F* and *P* values for the main effects and their interactions. An asterisk (*) indicates significance at the α = 0.05 level

SS sum of squares, *MS* mean squares, DF_{Num} numerator degrees of freedom, DF_{Den} denominator degrees of freedom

[1]Log-transformed data

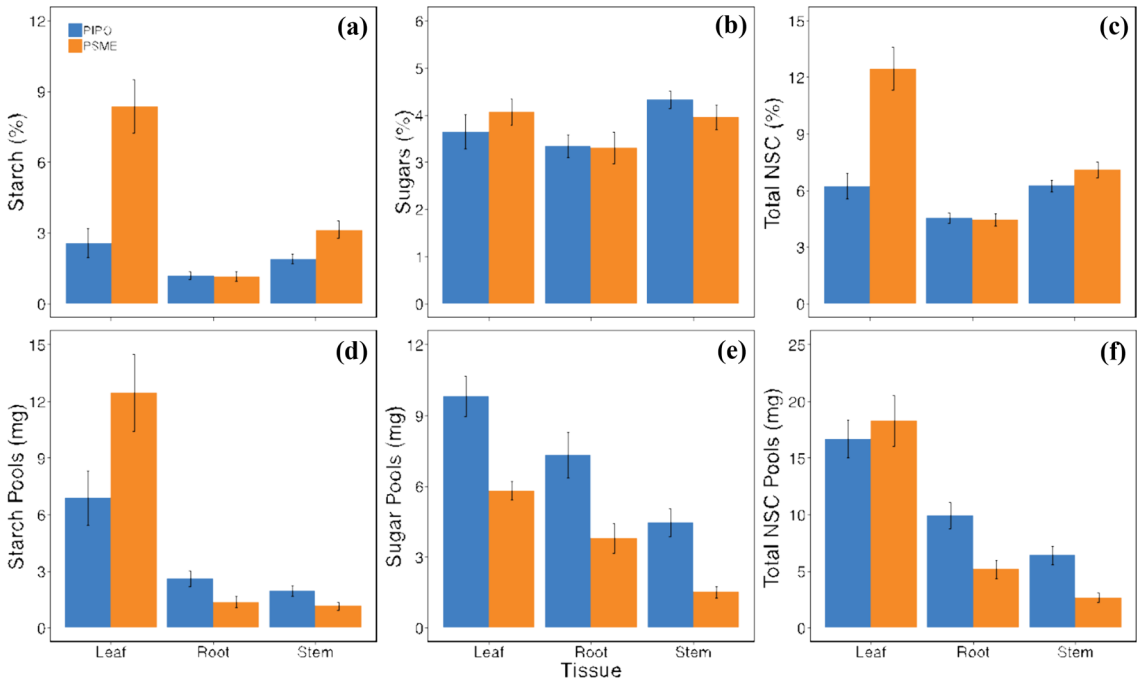

Fig. 5 Nonstructural carbohydrate (NSC) concentrations (%) and pools (mg) measured for both treatments combined in PIPO and PSME on DOY 247. Shown are mean (±1 SEM) % starch (**a**), % sugars (**b**), % total NSC (**c**), starch pools (**d**), sugar pools (**e**), and total NSC pools (**f**) for leaves, roots, and stems. Corresponding statistics are shown in Table 7

to consistently maintain higher mean values of seedling water potential during both predawn and mid-day periods, and under both drought and control conditions than PSME (Fig. 1c, d). Consistent with the results of Garcia-Forner et al. (2016) in which survival of *Pinus sylvestris* seedlings during extreme drought was highly positively correlated with carbon uptake, PIPO in this study maintained significantly higher rates of photosynthesis and stomatal conductance than PSME (Fig. 4) (Marias et al. 2017). This suggests that PIPO was able to maintain higher seedling water potential via some other means than by maintaining a more conservative stomatal control of transpiration. The significantly greater root mass in PIPO (Fig. 2c) is likely to have increased its ability to survive drought conditions by providing access to greater soil moisture availability in the raised beds and enabling higher rates of gas exchange. This rooting biomass advantage appears to have originated very early on (Fig. 2c) and was likely achieved not only by higher photosynthetic and growth rates, but also due to PIPO having a significantly larger seed size with a mean value 0.054 g, compared to a mean PSME seed mass of 0.012 g ($p = < 0.000001$, data not shown). The significantly larger root and stem NSC pools in PIPO than PSME were at least in part attributable to the significantly larger biomass values in those components relative to PSME (Figs. 2 and 5).

To further identify mechanisms associated with the relatively high levels of mortality in PSME, we examined the NSC dynamics of seedlings that had either recently died or were in the process of dying. The largely non-significant differences in total NSC concentrations and pools between healthy and dead/dying PSME seedlings (Fig. 6c, d), as well as the relatively minimal impact of drought on gas exchange (Fig. 4) and seedling maximum hydraulic conductivity, suggest that carbon acquisition at the whole-seedling level did not drive the differences in growth and mortality across treatments within PSME. The significantly lower NSC concentrations and pools in the roots of the dead/dying PSME seedlings compared with the healthy seedlings, along with their significantly higher NSC concentrations and pools in their stems compared with the healthy seedlings (Fig. 6), may provide insight into mechanisms involved in PSME seedling mortality in this study. It is possible that within seedlings that were dead/dying, carbon resources were preferentially allocated above ground to bolster carbon assimilation, consequently leading to some level of carbon depletion in the roots. Sugars in the leaves and shoots could have reduced the osmotic potential of the cells and maintained positive turgor pressure, which is required for healthy physiological functioning. Preferential allocation of NSC above ground may have also ensured a gradient in water potential from the soil to the leaves, which would drive water flow along that path. Consistent with this explanation are the data showing gas exchange was maintained in the drought-treated individuals, which is consistent with

Table 7 Linear mixed effects models comparing nonstructural carbohydrate (NSC) concentrations and NSC pools across water treatments (Water), tissue type (Tissue), species, and their interactions, as well seedling population (Population)

Variable	SS	MS	DF_{Num}	DF_{Den}	F	*P*
NSC concentrations						
Total NSC[1]						
Water	0.06	0.06	1	27.48	1.15	0.29
Tissue	6.31	3.16	2	54.07	57.77	< 0.01*
Species	0.77	0.77	1	27.48	14.07	< 0.01*
Population	0.004	0.004	1	27.35	0.06	0.80
Water * Tissue	0.06	0.03	2	54.07	0.51	0.60
Water * Species	0.09	0.09	1	27.48	1.65	0.21
Tissue * Species	2.34	1.17	2	54.07	21.40	< 0.01*
Water * Tissue * Species	0.29	0.14	2	54.07	2.62	0.08
Starch[1]						
Water	0.05	0.05	1	2.01	0.18	0.72
Tissue	20.98	10.49	2	52.82	39.89	< 0.01*
Species	5.70	5.70	1	25.19	21.68	< 0.01*
Population	0.02	0.02	1	25.22	0.07	0.79
Water * Tissue	0.57	0.28	2	52.86	1.08	0.35
Water * Species	0.03	0.03	1	25.21	0.12	0.73
Tissue * Species	6.02	3.01	2	52.84	11.44	< 0.01*
Water * Tissue * Species	1.00	0.50	2	52.86	1.89	0.16
Sugars						
Water	1.11	1.11	1	2.01	1.61	0.33
Tissue	10.58	5.29	2	53.59	7.72	< 0.01*
Species	0.01	0.01	1	24.88	0.01	0.91
Population	0.001	0.001	1	24.79	0.002	0.97
Water * Tissue	4.22	2.11	2	53.59	3.08	0.05
Water * Species	1.58	1.58	1	24.88	2.31	0.14
Tissue * Species	2.96	1.48	2	53.59	2.16	0.13
Water * Tissue * Species	2.65	1.32	2	53.59	1.93	0.16
NSC pools						
Total NSC[1]						
Water	0.04	0.04	1	2.01	0.23	0.68
Tissue	35.13	17.57	2	52.51	91.76	< 0.01*
Species	2.46	2.46	1	24.53	12.83	< 0.01*
Population	0.23	0.23	1	24.44	1.18	0.29
Water * tissue	0.18	0.09	2	52.51	0.46	0.63
Water * species	0.04	0.04	1	24.53	0.20	0.66
Tissue * species	4.14	2.07	2	52.51	10.81	< 0.01*
Water * tissue * species	0.81	0.41	2	52.51	2.12	0.13
Starch[1]						
Water	0.001	0.001	1	2.01	0.003	0.96
Tissue	55.95	27.97	2	51.98	76.81	< 0.01*
Species	0.15	0.15	1	25.17	0.41	0.53
Population	0.30	0.30	1	25.19	0.82	0.37
Water * Tissue	0.08	0.04	2	52.01	0.12	0.89
Water * Species	0.01	0.01	1	25.18	0.03	0.87
Tissue * Species	8.17	4.08	2	52.02	11.21	< 0.01*
Water * Tissue * Species	2.72	1.36	2	52.03	3.74	0.03*
Sugars[2]						
Water	0.16	0.16	1	2.02	0.71	0.49
Tissue	19.61	9.80	2	52.64	43.95	< 0.01*
Species	6.57	6.57	1	24.61	29.44	< 0.01*

Table 7 (continued)

Variable	SS	MS	DF_{Num}	DF_{Den}	F	*P*
Population	0.04	0.04	1	24.51	0.18	0.67
Water * Tissue	0.2	0.14	2	52.64	0.62	0.54
Water * Species	0.08	0.08	1	24.61	0.36	0.55
Tissue * Species	0.16	0.08	2	52.64	0.35	0.71
Water * Tissue * Species	0.10	0.05	2	52.64	0.24	0.79

Bed and position within bed were included as random effects for all analyses, *F* and *P* values for the main effects and their interactions. An asterisk (*) indicates significance at the $\alpha = 0.05$ level

SS Shown are sum of squares, *MS* mean squares, DF_{Num} numerator degrees of freedom, DF_{Den} denominator degrees of freedom

[1]Log-transformed data

[2]Square root-transformed data

maintenance of turgor pressure, and with water potentials being reduced by the drought treatment. A second hypothesis is that mycorrhizal fungi associated with the roots of the dead/dying seedlings may have switched from being mutualistic to parasitic towards the end of the study (Jones and Smith 2004; Ibáñez and McCarthy-Neumann, 2016); however, this does not explain the significantly higher levels of NSC in the leaves and stems of dead/dying seedlings. A third possibility is that the dead/dying seedlings experienced constraints on the transport of NSC from foliage to roots and that carbon starvation contributed to their mortality. Water stress can lead to constraints on turgor-driven cell expansion (Hsiao 1973), producing narrower conduits which cause constraints on transport within the xylem (Anfodillo et al. 2012) and phloem (Woodruff et al. 2014). In addition to constraints associated with reduced conduit size, phloem transport limitation can also involve the impacts of water stress on phloem sap viscosity, because viscosity is influenced by the relative concentrations of water and solutes (Darcy's law), such as sugars within the phloem sap, and the axial phloem sap inflow rate of phloem sieve elements is inversely related to sap viscosity (Münch 1930, Hölttä et al. 2006). This explanation is consistent with results from Sevanto et al. (2014) in which accessibility and consumption rate of carbohydrate stores were critical to survival of droughted *Pinus edulis*. This hypothesis is also consistent with results from Rehschuh et al. (2021) who found a 40% lower translocation velocity of ^{13}C labeled carbon in *Pinus sylvestris* seedlings recovering from drought-heat compared with control seedlings.

Mean root mass of the dead/dying PSME seedlings was approximately half that of the healthy seedlings (0.062 g, se = 0.004 vs. 0.116 g, se = 0.014, respectively, data not shown), suggesting that root growth was likely impaired by low carbon availability in PSME. The sizes of these seedlings during such early stages of development means that the transport of NSC from one organ to another (such as from foliage to roots) could occur over relatively small distances, and the pools of NSC within different seedling components represent an important indicator of potential source and sink relationships. The substantially lower mean root NSC concentration and pool size in the dead/dying seedlings, along with the substantially higher mean stem NSC concentration and pool size in the healthy seedlings (Fig. 6) suggests that the decline and mortality of these seedlings could be associated with constraints on phloem transport to roots, which is consistent with water stress reducing phloem cell size and by increasing phloem sap viscosity (Woodruff 2014). Our findings showing a substantially greater depletion of NSC in roots than in above ground components under conditions of water stress are also consistent with Hartmann et al. (2013), who examined carbon and water relations during drought-induced mortality in 7-year-old *Picea abies* (L.) Karst. They found that NSC concentrations in droughted needles and branches were similar to those of control trees. Root NSC concentrations, however, were reduced in the drought treatment and starch was almost completely depleted in droughted roots. Similarly, Klein et al. (2014) examined growth and NSC dynamics of mature *Pinus halepensis* Mill. trees exposed to a range of drought stress levels and observed lower root NSC and higher branch NSC in stressed and non-stressed trees consistent with the healthy and dead/dying seedlings in the current study. Although in that study both starch and sugar content in branches were similar across three levels of water stress, root starch levels in moderately stressed and stressed trees were 47% and 58% of healthy trees, respectively. In a study examining mortality of young *Pinus flexilis* E.James seedlings grown beyond the warm edge of their natural range, Reinhardt et al. (2015) found low below-ground and high above-ground late-season NSC content. They proposed that interruption of phloem transport was a key factor in seedling mortality for their study, in which all eventually died at the end of the growing season. However, Garcia-Forner et al. (2016) found an across the board reduction in branch, root and stem NSC concentrations in *Pinus sylvestris* seedlings that had died

Table 8 Linear mixed effects models comparing nonstructural carbohydrate (NSC) concentrations and NSC pools across water treatments (Water), tissue type (Tissue), health status (Health), and their interactions, as well seedling population (Population), for PSME only

Variable	SS	MS	DF_{Num}	DF_{Den}	F	*P*
NSC Concentrations						
Total NSC[2]						
Water	0.23	0.23	1	1.80	0.80	0.48
Tissue	90.24	45.12	2	99.65	157.55	< 0.01*
Health	0.03	0.03	1	100.15	0.11	0.74
Population	0.33	0.33	1	15.95	1.16	0.30
Water * Tissue	0.29	0.15	2	99.73	0.51	0.60
Water * Health	0.06	0.06	1	96.57	0.21	0.65
Tissue * Health	18.77	9.39	2	99.06	32.78	< 0.01*
Water * Tissue * Health	0.19	0.09	2	99.07	0.33	0.72
Starch[2]						
Water	0.004	0.004	1	1.78	0.01	0.94
Tissue	57.39	28.70	2	112.01	59.97	< 0.01*
Health	1.17	1.17	1	111.43	2.44	0.12
Population	2.61	2.61	1	114.00	5.46	0.02*
Water * Tissue	0.01	0.01	2	112.00	0.01	0.99
Water * Health	0.01	0.01	1	112.49	0.02	0.88
Tissue * Health	4.56	2.28	2	112.06	4.76	0.01*
Water * Tissue * Health	0.11	0.06	2	112.04	0.12	0.89
Sugars[2]						
Water	0.30	0.30	1	1.96	1.95	0.30
Tissue	30.05	15.02	2	101.02	99.17	< 0.01*
Health	1.29	1.29	1	101.26	8.54	< 0.01*
Population	0.35	0.35	1	17.35	2.32	0.15
Water * Tissue	0.77	0.38	2	101.09	2.54	0.08
Water * Health	0.03	0.03	1	97.69	0.22	0.64
Tissue * Health	18.23	9.11	2	100.47	60.15	< 0.01*
Water * Tissue * Health	0.13	0.06	2	100.48	0.42	0.66
NSC Pools						
Tissue NSC pools[1]						
Water	0.62	0.62	1	1.79	1.27	0.39
Tissue	85.48	42.74	2	72.92	88.30	< 0.01*
Health	0.16	0.16	1	1.86	0.33	0.63
Population	0.30	0.15	2	27.29	0.31	0.73
Water * Tissue	1.67	0.83	2	72.95	1.72	0.19
Water * Health	0.06	0.06	1	27.05	0.11	0.74
Tissue * Health	27.85	13.92	2	72.92	28.77	< 0.01*
Treatment * Tissue * Health	0.60	0.30	2	72.95	0.62	0.54
Whole-plant NSC pools[2]						
Water	0.63095	0.63095	1	1.6418	0.44	0.59
Health	0.59961	0.59961	1	0.3692	0.42	0.74
Population	0.03867	0.01933	2	2	0.01	0.99
Water * Health	0.01707	0.01707	1	13.8728	0.01	0.91

Also shown is a separate analysis comparing whole-plant NSC pools across treatments, health status, their interactions, as well as seedling population. Bed, position within bed, and sampling date were included as random effects for all analyses, *F* and *P* values for the main effects and their interactions. An asterisk (*) indicates significance at the $\alpha = 0.05$ level

SS sum of squares, *MS* mean squares, DF_{Num} numerator degrees of freedom, DF_{Den} denominator degrees of freedom

[1]Log-transformed data

[2]Square root-transformed data

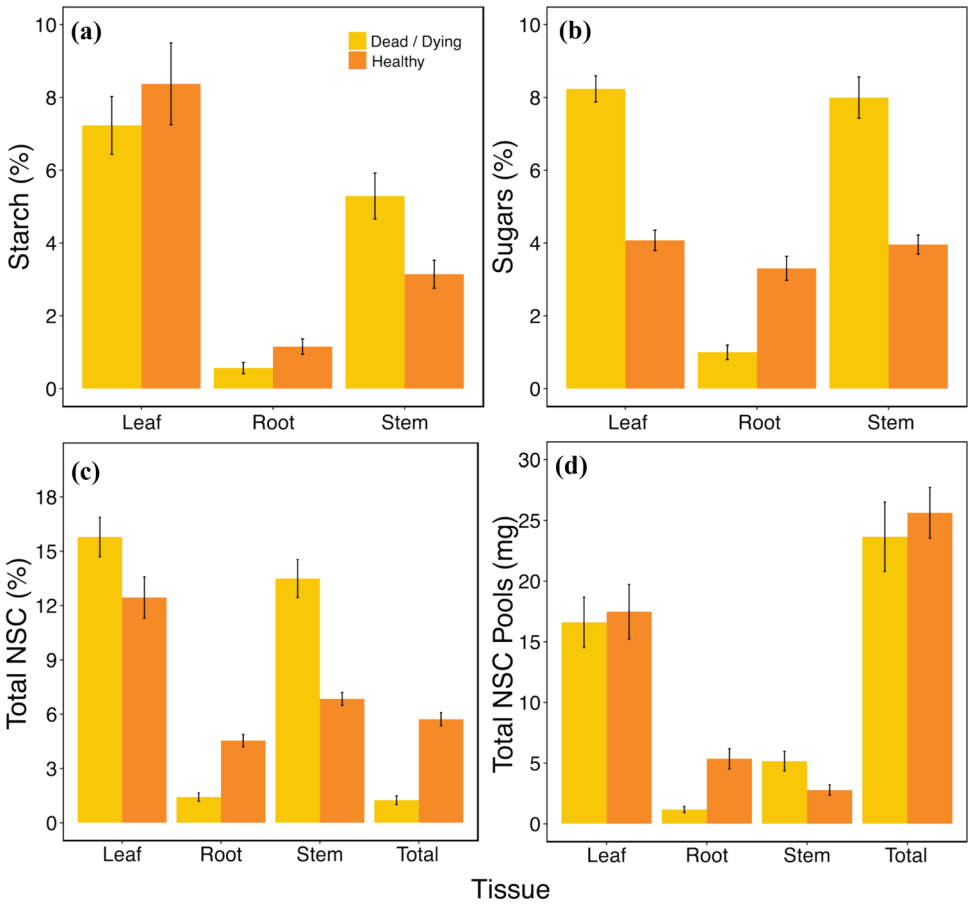

Fig. 6 Nonstructural carbohydrate (NSC) concentrations (%) and pools (mg) measured for healthy vs. dead/dying PSME. Shown are mean (± 1 SEM) % starch (**a**) and % sugars (**b**) for leaves, roots, and stems, as well as total NSC (**c**) and total NSC pools (**d**) for leaves, roots, stems, and whole plants ("Total") measured in healthy and dead/dying individuals. Corresponding statistics are shown in Table 8

from drought, relative to surviving seedlings, indicating that organs do not always differ in their NSC content in response to drought.

A potential impact of climate change is the shifting of tree species distributions, especially in temperate forests such as those representing much of the range of the two study species. The greater survival of PIPO seedlings, particularly under drought conditions, may mean greater establishment of this species and lower establishment of PSME in areas previously favorable to PSME, which may be driven by the differential physiological functioning and survival of young seedlings. The observed patterns of water depletion at different depths in the drought treatment, along with the differences in root biomass between species, highlight the critical role of early root development in growth and survival. The distinct differences between species in gas exchange, coupled with the minimal response within species to drought, highlights the potential role of gas exchange in PIPO's advantage of PSME at this key developmental stage. The pronounced patterns of NSC accumulation and depletion in declining PSME seedlings suggests a potentially important mechanism involved in mortality during early stages of development and establishment, possibly involving either osmotic adjustment or drought-related constraints on phloem transport. Further research examining growth and survival responses of different tree species to drought stress during early stages of development is necessary to more accurately predict future changes in species distributions. Emphases on physiological processes including osmotic adjustment and phloem transport could provide additional insights into the underlying mechanisms of seedling mortality and which characteristics are most influential for survival and establishment following germination.

Acknowledgements The authors thank Brad St Clair, Rich Cronn, Jeff Riddle and Chris Poklemba, USDA Forest Service, PNW Research Station for providing seed material and for advice concerning seed sources and seed stratification and germination, Larry Miller, Oregon Department of Forestry for providing seed material, and the USDA Forest Service, PNW Research Station for providing facilities plus funding and Alicia Magedman for lab help. We would also like to thank Cécile Ane for her generous advice concerning statistical methods.

Author contribution DW, FM and KM conceived of the study. Statistical analyses were done by KO in conjunction with DW. DW, FM, KM, KK, DU and JC contributed to collecting samples and conducting field measurements. DW conducted the carbohydrate analyses. DW wrote

the initial draft and all authors contributed to manuscript editing and approved the final manuscript.

Funding This work was supported by NSF grant IOS 11-46746 and the USDA Forest Service, Pacific Northwest Research Station.

Declarations

Conflict of interest None declared.

References

Abramoff MD, Magelhaes PJ, Ram SJ (2004) Image Processing with Image. J Biophotonics Int 11:36–42

Anfodillo T, Deslauriers A, Menardi R, Tedoldi L, Petit G, Rossi S (2012) Widening of xylem conduits in a conifer tree depends on the longer time of cell expansion downwards along the stem. J Exp Bot 63:837–845

Araújo MB, Rahbek C (2006) How does climate change affect biodiversity? Science 313:1396–1397

Brubaker LB (1986) Responses of tree populations to climatic change. Vegetatio 67:119–130

Burns RM, Honkala BH (1990) Silvics of North America, vol 2. US Department of Agriculture, Forest Service, Washington, DC, USA

Chmura DJ, Anderson PA, Howe GT, Harrington CA, Halofsky JE, Peterson DL, Shaw DC, St. Clair JB (2011) Forest responses to climate change in the northwestern United States: ecophysiological foundations for adaptive management. For Ecol Manag 261:1121–1142

Domec JC, Gartner BL (2002) How do water transport and water storage differ in coniferous earlywood and latewood? J Exp Bot 53:2369–2379

Dyderski MK, Paź S, Frelich LE, Jagodziński AM (2018) How much does climate change threaten European forest tree species distributions? Global Change Biol 24(3):1150–1163

Engelbrecht BMJ, Comita LS, Condit R, Kursar TA, Tyree MT, Turner BL, Hubbell SP (2007) Drought sensitivity shapes species distribution patterns in tropical forests. Nature 447:80–82

Eriksson O, Ehrlén J (2008) Seedling recruitment and population ecology. In: Leck M, Parker V, Simpson R (eds) Seedling ecology and evolution. Cambridge University Press, Cambridge, pp 239–254

Faraway J (2005) Linear Models with R. Chapman and Hall, London

Franklin JF, Dyrness CT (1988) Natural vegetation of Oregon and Washington. Oregon State University Press, Corvallis, OR, p 452

Garcia-Forner N, Sala A, Biel C, Savé R, Martínez-Vilalta J (2016) Individual traits as determinants of time to death under extreme drought in *Pinus sylvestris* L. Tree Physiol 36:1196–1209

Gentry AH (1988) Changes in plant community diversity and floristic composition on environmental and geographical gradients. Ann Missouri Bot Gard 75(1):1–34

Gougherty AV, Keller SR, Fitzpatrick MC (2021) Maladaptation, migration and extirpation fuel climate change risk in a forest tree species. Nat Clim Change 11:166–171. https://doi.org/10.1038/s41558-020-00968-6

Harrison XA, Donaldson L, Correa-Cano ME, Evans J, Fisher DN, Goodwin CE, Robinson BS, Hodgson DJ, Richard I (2018) A brief introduction to mixed effects modelling and multi-model inference in ecology. PeerJ 6:e4794

Hartmann H, Trumbore S, Ziegler W (2013) Lethal drought leads to reduction in nonstructural carbohydrates (NSC) in Norway spruce tree roots but not in the canopy. Funct Ecol 27:413–427

Hartshorn GS (1972) The ecological life history and population dynamics of *Pentaclethra macroloba*, a tropical wet forest dominant and *Stryphnodendron excelsum*, an occasional associate. Ph.D. thesis, University of Washington, Seattle. 119 p.

Hoch G, Richter A, Körner C (2003) Non-structural carbon compounds in temperate forest trees. Plant Cell Environ 26:1067–1081

Hölttä T, Vesala T, Sevanto S, Perämäki M, Nikinmaa E (2006) Modeling xylem and phloem water flows in trees according to cohesion theory and Münch hypothesis. Trees 20:67–78. https://doi.org/10.1007/s00468-005-0014-6

Hsiao TC (1973) Plant responses to water stress. Annu Rev Plant Physiol 24:519–570

Ibáñez, I, S. McCarthy-Neumann (2016) Effects of mycorrhizal fungi on tree seedling growth: quantifying the parasitism–mutualism transition along a light gradient. Can J Res 46:48–57

IPCC (2022) Climate change 2022: impacts, adaptation, and vulnerability. Contribution of working group II to the sixth assessment report of the intergovernmental panel on climate change. In: H-O Pörtner, DC Roberts, M Tignor, ES Poloczanska, K Mintenbeck, A Alegría, M Craig, S Langsdorf, S Löschke, V Möller, A Okem, B Rama (Eds.). Cambridge University Press, Cambridge, UK and New York, NY, USA, p. 3056

Jones MD, Smith SE (2004) Exploring functional definitions of mycorrhizas: are mycorrhizas always mutualisms? Can J Bot 82(8):1089–1109

Kerr K, Meinzer FC, McCulloh KA, Woodruff DR, Marias DE (2015) Expression of functional traits during seedling establishment in two populations of Pinus ponderosa from contrasting climates. Tree Physiol 35:535–548

Klein T, Yakir D, Hoch G (2014) Drought stress, growth, and nonstructural carbohydrate dynamics of pine trees in a semi-arid forest. Tree Physiol 34:981–992

Little EL (1971) Atlas of United States trees. Conifers and important hardwoods. Miscellaneous publication 1146. Washington, DC: U.S. Department of Agriculture, Forest Service 1:320

Lusk CH, Piper FI (2007) Seedling size influences relationships of shade tolerance with carbohydrate-storage patterns in a temperate rainforest. Funct Ecol 21(1):78–86

Maguire AJ, Kobe RK (2015) Drought and shade deplete nonstructural carbohydrate reserves in seedlings of five temperate tree species. Ecol and Evolution 5:5711–5721

Marias DE, Meinzer FC, Woodruff DR, McCulloh KA (2017) Thermotolerance and heat stress responses of Douglas-fir and ponderosa pine seedling populations from contrasting climates. Tree Physiol 37:301-315

Martinez-Vilalta J, Sala A, Piñol J (2004) The hydraulic architecture of pinaceae—a review. Plant Ecol 171:3–13

McMinn RG (1952) The role of soil drought in the distribution of vegetation in the northern Rocky Mountains. Ecol. 33:1–15

Meehl GA, Tebaldi C (2004) More intense, more frequent, and longer-lasting heat waves in the 21st century. Science 305:994–997

Münch E (1930) Die Stoffbewegungen in der Pflanze. Verlag von Gustav Fischer, Jena, p 234

Nardini A, Casolo V, Dal Borgo A, Savi T, Stenni B, Bertoncin P, Zini L, McDowell NG (2016) Rooting depth, water relations and non-structural carbohydrate dynamics in three woody angiosperms differentially affected by an extreme summer drought. Plant Cell Environ 39:618–627

Ovalle JF, Arellano EC, Ginocchio R (2015) Trade-offs between drought survival and rooting strategy of two South American Mediterranean tree species: implications for dryland forests restoration. Forests 6:3733–3747

Padilla FM, Pugnaire FI (2007) Rooting depth and soil moisture control Mediterranean woody seedling survival during drought. Funct Ecol 21:489–495

Parmesan C (2006) Ecological and evolutionary responses to recent climate change. Annu Revi Ecol Evol Syst 37:637–669

Piñero D, Martínez-Ramos MM, Sarukhán J (1984) A population model of Astocaryum mexicanum and a sensitivity analysis of its finite rate of increase. J Ecol 72:977–991

Piñol J, Sala A (2000) Ecological implications of xylem cavitation for several pinaceae in the Pacific Northwest. Funct Ecol 14:538–545

R Core Team (2017) R: a language and environment for statistical computing. https://www.R-project.org/

Rehschuh R, Rehschuh S, Gast A, Jakab AL, Lehmann MM, Saurer M, Gessler A, Ruehr NK (2022) Tree allocation dynamics beyond heat and hot drought stress reveal changes in carbon storage, belowground translocation and growth. New Phyt 233:687–704

Reinhardt K, Germino MJ, Kueppers LM, Domec J-C, Mitton J, Ryan M (2015) Linking carbon and water relations to drought-induced mortality in *Pinus flexilis* seedlings. Tree Physiol 35:771–782

Scheller RM, Mladenoff DJ (2005) A spatially interactive simulation of climate change, harvesting, wind, and tree species migration and projected changes to forest composition and biomass in northern Wisconsin, USA. Glob Chang Biol 11:307–321

Seager R, Ting M, Held I, Kushnir Y, Lu J, Vecchi G, Huang HP, Harnik N, Leetmaa A, Lau NC, Li C, Velez J, Naik N (2007) Model projections of an imminent transition to a more arid climate in southwestern North America. Science 316:1181–1184

Sevanto S, McDowell NG, Dickman LT, Pangle R, Pockman WT (2014) How do trees die? A test of the hydraulic failure and carbon starvation hypotheses. Plant Cell Environ 37:153–161

Stout DL, Sala A (2003) Xylem vulnerability to cavitation in Pseudotsuga meinziesii and Pinus ponderosa from contrasting habitats. Tree Physiol 23:43–50

Teskey R, Wertin T, Bauweraerts I, Ameye M, McGuire MA, Steppe K (2015) Responses of tree species to heat waves and extreme heat events Plant Cell Environ 38 (2015):1699–1712

Urli M, Perie C, Thiffault N (2023) Experimental drier climates affect hydraulics and induce high mortality of seedlings of three northern conifer species. For Ecol Manag 544(11):121127. https://doi.org/10.1016/j.foreco.2023.121127

Woodruff DR (2014) The impacts of water stress on phloem transport in Douglas-fir trees. Tree Physiol 34:5–14

Woodruff DR, Meinzer FC (2011) Water stress, shoot growth and storage of nonstructural carbohydrates along a tree height gradient in a tall conifer. Plant Cell Environ 11:1920–1930

Yuan X, Wang Y, Wu P, Sheffield J, Otkin J (2023) A global transition to flash droughts under climate change. Science. https://doi.org/10.1126/science.abn6301